DALTON
FULL PAPER

Organically templated linear and layered cadmium sulfates†

Geo Paul,[a] Amitava Choudhury[a,b] and C. N. R. Rao*[a,b]

[a] *Chemistry and Physics of Materials Unit, Jawaharlal Nehru Centre for Advanced Scientific Research, Jakkur P.O., Bangalore, 560 064, India. E-mail: cnrrao@jncasr.ac.in*
[b] *Solid State and Structural Chemistry Unit, Indian Institute of Science, Bangalore, 560 012, India*

Received 9th May 2002, Accepted 31st July 2002
First published as an Advance Article on the web 13th September 2002

By reacting cadmium salts with H_2SO_4 in the presence of organic amines or directly with amine sulfates under hydrothermal conditions, it has been possible to prepare three linear cadmium sulfates of linarite topology, with the compositions $[H_3N(CH_2)_2NH_3]_2[CdCl_2(SO_4)][SO_4]\cdot H_2O$, **I**, $[HN(CH_2)_6NH][CdBr_2(SO_4)]$, **II**, $[HN(CH_2)_6NH][CdCl_2(SO_4)]$, **III**. A layered cadmium sulfate of composition $[H_3N(CH_2)_3NH_3][Cd_2(H_2O)_2(SO_4)_3]$, **IV**, has also been obtained. These sulfates are the first examples of a family of organically templated metal sulfates with interesting structural features. In the linarite chains, the CdX_4O_2 (X = Cl, Br) octahedron shares two *trans*-edges to form an $[M\varphi_4]$ (φ = anionic ligand) chain decorated by the SO_4 tetrahedron that adopts a staggered arrangement on either side of the chain. **IV** is constructed by the fusion of four-membered ring ladders involving edge sharing between the sulfate tetrahedron and metal octahedron. **IV** appears to be the first member of a family of organically templated metal sulfates containing an octahedral–tetrahedral 2D net wherein the sulfate tetrahedron is connected at all four corners.

Introduction

Besides the open-framework aluminosilicates,[1] metal phosphates constitute a large class of inorganic open-framework architectures.[2] Open-framework metal phosphates include not only three-dimensional (3D) structures with channels but also structures with two-dimensional (2D) layers and one-dimensional (1D) chains.[3] Recently, there has been growing interest in the study of open-framework architectures containing oxo anions of sulfur and selenium.[4] We have been exploring the possibility of synthesizing open-framework structures wherein the sulfate tetrahedron acts as the primary building unit instead of the phosphate tetrahedron. Since the use of structure-directing organic molecules has evolved into a successful strategy for the synthesis of layered and zeolitic materials, we sought to expand the metal sulfate family of solids by the introduction of various organoammonium cations as templates in the hydrothermal preparation of the sulfates. Towards this end, we have carried out hydrothermal reactions of cadmium salts in the presence of H_2SO_4 and organic amines and have obtained cadmium sulfates possessing layered and linarite-like chain structures. In this article, we describe the structural features of three chain compounds, $[H_3N(CH_2)_2NH_3]_2[CdCl_2(SO_4)][SO_4]\cdot H_2O$, **I**, $[HN(CH_2)_6NH][CdBr_2(SO_4)]$, **II**, $[HN(CH_2)_6NH][CdCl_2(SO_4)]$, **III**, and one layered compound, $[H_3N(CH_2)_3NH_3][Cd_2(H_2O)_2(SO_4)_3]$, **IV**. Besides being the first such examples of cadmium sulfates these materials are also the first members of a family of organically templated open-framework metal sulfates. This article also demonstrates the occurrence of octahedral–tetrahedral four-connected two-dimensional nets formed by the fusion of four-membered ring ladders.[5]

† Electronic supplementary information (ESI) available: powder diffraction data for **IV**, view of **I** down the *a*-axis, the structure of **II** in the *ac*-plane and a polyhedral view of **IV** in the *ab*-plane. See http://www.rsc.org/suppdata/dt/b2/b204482j/

Experimental

Compounds **I** to **IV** were synthesized by employing mild hydro/solvothermal methods.

$[H_3N(CH_2)_2NH_3]_2[CdCl_2(SO_4)][SO_4]\cdot H_2O$, I

In a typical synthesis 0.2013 g of $CdCl_2\cdot H_2O$ was dissolved in a butan-2-ol/H_2O mixture (2.8 mL/0.54 mL) under constant stirring. To this solution, was added 0.4743 g of $[H_3N(CH_2)_2NH_3]\cdot SO_4$ (ENS) and the mixture stirred for 30 minutes to obtain a homogeneous gel. The final mixture with a molar composition of $1CdCl_2\cdot H_2O$: 4ENS : 30butan-2-ol : $30H_2O$ was transferred into a 23mL PTFE-lined acid digestion bomb and heated at 100 °C for 48 h. The product contained colorless rod-like crystals which were monophasic (yield 68%, with respect to Cd).

$[HN(CH_2)_6NH][CdBr_2(SO_4)]$, II

A solution of $Cd(OAc)_2\cdot 2H_2O$ (0.2665 g), DABCO (0.3365 g), H_2SO_4 (98%) (0.16 mL), HBr (49%) (0.22 mL), H_2O (1.8 mL) and butan-2-ol (9.4 mL) in the molar ratio, 1 : 3 : 3 : 2 : 100 : 100 was heated in a polypropylene bottle at 100 °C for 48 h. After cooling to room temperature colorless plate-like crystals of **II** were isolated in 65% yield.

$[HN(CH_2)_6NH][CdCl_2(SO_4)]$, III

A solution of $CdCl_2\cdot H_2O$ (0.2013 g), $(NH_4)_2SO_4$ (0.5285 g), DABCO (0.3365 g), H_2O (0.54 mL) and butan-2-ol (2.8 mL) in the molar ratio, 1 : 4 : 3 : 30 : 30 was transferred into a 23 mL PTFE-lined stainless steel autoclave and stirred for 10 min. Finally 0.5 mL of 5 M H_2SO_4 was added and the container sealed and kept at 150 °C for 48 h. After cooling to room temperature colorless rod shaped crystals of **III** were isolated in 60% yield.

Table 1 Crystal data and structure refinement parameters for **I**–**IV**

Structural parameter	**I**	**II**	**III**	**IV**
Empirical formula	$C_4H_{22}CdCl_2N_4O_9S_2$	$C_{1.5}H_{3.5}Cd_{0.25}Br_{0.5}N_{0.5}OS_{0.25}$	$C_{1.5}H_{3.5}Cd_{0.25}Cl_{0.5}N_{0.5}OS_{0.25}$	$C_3H_{16}Cd_2N_2O_{14}S_3$
Crystal system	Orthorhombic	Orthorhombic	Orthorhombic	Triclinic
Space group	$P2_12_12_1$	*Cmcm*	*Cmcm*	$P\bar{1}$
a/Å	7.3207(2)	9.7782(9)	9.7138(10)	8.3802(4)
b/Å	10.6852(3)	17.300(2	16.922(2)	8.6579(5)
c/Å	21.8939(3)	7.5504(7)	7.3872(8)	11.3254(6)
α/°	90	90	90	84.926(2)
β/°	90	90	90	72.414(2)
γ/°	90	90	90	75.741(2)
Volume/Å^3	1712.61(7)	1277.3(2)	1214.3(2)	759.09(7)
Z	4	16	16	2
Formula mass	517.68	120.62	98.39	625.16
μ/mm^{-1}	1.876	8.130	2.410	3.292
Total data collected	7148	2636	2520	3176
Unique data	2461	533	510	2150
R_{int}	0.0311	0.0314	0.0434	0.0330
R (all data)	$R_1 = 0.0287$,[a] $wR_2 = 0.0507$[b]	$R_1 = 0.0244$,[a] $wR_2 = 0.0600$[b]	$R_1 = 0.0260$,[a] $wR_2 = 0.0663$[b]	$R_1 = 0.0494$,[a] $wR_2 = 0.0855$[b]

[a] $R_1 = \Sigma||F_o| - |F_c|| / \Sigma|F_o|$. [b] $wR_2 = \{[w(F_o^2 - F_c^2)^2] / [w(F_o^2)^2]\}^{1/2}$, $w = 1 / [\sigma^2(F_o)^2 + (aP)^2 + bP]$, $P = [F_o^2 + 2F_c^2] / 3$; where $a = 0.0158$ and $b = 0.8553$ for **I**; $a = 0.0401$ and $b = 1.8302$ for **II**; $a = 0.0307$ and $b = 2.4096$ for **III**; $a = 0.0322$ and $b = 0$ for **IV**.

$[H_3N(CH_2)_3NH_3][Cd_2(H_2O)_2(SO_4)_3]$, IV

In a typical synthesis 1.066 g of $Cd(OAc)_2{\cdot}2H_2O$ was dispersed in an ethylene glycol/H_2O mixture (11.2 mL/3.6 mL) under constant stirring. To this solution, was added 0.3444 g of $[H_3N(CH_2)_3NH_3]{\cdot}[SO_4]$ (DAPS) and 0.16 mL H_2SO_4(98%) and the mixture stirred for 5 minutes. The final mixture with a molar composition of $4Cd(OAc)_2{\cdot}2H_2O$: 2DAPS : $3H_2SO_4$: $200H_2O$: 200ethylene glycol was transferred to a polypropylene bottle, sealed and heated at 100 °C for 48 hours to obtain colorless plate-type crystals (yield 40%).

The organoammonium sulfates, $[H_3N(CH_2)_2NH_3]{\cdot}SO_4$ (ENS) and $[H_3N(CH_2)_3NH_3]{\cdot}SO_4$ (DAPS) were prepared following the procedure reported in the literature.[6] In all four cases the initial pH of the reaction mixture was found to be around 2 and no appreciable change in the pH was noted after the reaction. EDAX analysis indicated a Cd : S : Cl/Br ratio of 1 : 2 : 2 for **I**, 1 : 2 : 1 for **II**, 1 : 2 : 1 for **III** and 2 : 3 : 0 for **IV**.

I–**IV** gave satisfactory elemental analysis. The experimental and calculated (in wt%) values for C, H, N are as follows: **I**, C, 9.41; N, 10.85; and H, 4.37 (calc.: C, 9.27; N, 10.82; H, 4.25); **II**, C, 15.01; N, 5.83; and H, 3.24 (calc.: C, 14.92; N, 5.81; H, 2.90); **III**, C, 18.06; N, 6.77; and H, 3.53 (calc.: C, 18.30; N, 7.12; H, 3.56); **IV**, C, 5.68; N, 4.37; and H, 4.49; (calc.: C, 5.76; N, 4.48; H, 2.56%). Infrared (IR) spectra of **I**–**IV** show characteristic bands due to the sulfate ion in the 1100 and 618 cm^{-1} regions, besides bands due to C–H stretching and bending vibrations as well as those due to the amine moiety. A band around 3500 was found in **I** and **IV** due to the presence of water.

X-Ray crystallography

Suitable single crystals of all four compounds were carefully selected under a polarizing microscope and glued to a thin glass fibre with cyanoacrylate (superglue) adhesive. Single crystal data were collected on a Siemens SMART-CCD diffractometer [graphite-monochromated Mo-K_α radiation, λ = 0.71073 Å (T = 298K)]. An absorption correction based on symmetry-equivalent reflections was applied using SADABS.[7] The structures were solved by direct methods using SHELXS-86[8] and difference Fourier synthesis. The direct methods solution readily revealed the heavy atom positions (Cd, S, Cl and Br) and enabled us to locate the other non-hydrogen positions (O, C and N) from the difference Fourier maps. Hydrogen positions for both the bonded [O(5) and (O6) in **IV**] as well as the extra-framework water molecule [O(100) in **I**] were located from the difference Fourier map and placed in the observed position and refined isotropically. All the remaining hydrogen positions for **I**–**IV** were initially located in the difference Fourier maps, and for the final refinement, the hydrogen atoms were placed geometrically and held in the riding mode. The last cycles of refinement included atomic positions for all the atoms, anisotropic thermal parameters for all non-hydrogen atoms and isotropic thermal parameters for all the hydrogen atoms. Full-matrix least-squares structure refinement against $|F^2|$ was carried out using the SHELXTL-PLUS[9] package of programs. Details of the final refinement are given in Table 1. The powder X-ray diffraction patterns for all four compounds are in good agreement with the simulated pattern generated from the single crystal XRD data. A least-squares fit of the powder XRD (Cu-K_α) lines of the bulk sample of **IV**, using the *hkl* indices generated from single crystal X-ray data, gave the following cell: a = 8.37133, b = 8.64313, c = 11.30759 Å, α = 84.96043, β = 72.41003 and γ = 75.75724°, which is in good agreement with that determined by single crystal XRD. The powder diffraction data for **IV** are given as ESI† and the simulated and experimental powder patterns are presented in Fig. 1. Selected bond distances for compounds **I** to **III** and selected bond angles and distances for compound **IV** are listed in Tables 2 and 4 to 6 respectively. The various hydrogen bond interactions for **I** to **IV** are given in Table 3.

CCDC reference numbers 185728–185731.

See http://www.rsc.org/suppdata/dt/b2/b204482j/ for crystallographic data in CIF or other electronic format.

Results

$[H_3N(CH_2)_2NH_3]_2[CdCl_2(SO_4)][SO_4]{\cdot}H_2O$, I

The asymmetric unit of **I** contains 22 non-hydrogen atoms of which 13 belong to the inorganic framework, with one crystallographically distinct cadmium and two distinct sulfur atoms [Fig. 2(a)]. The structure is built up of isolated infinite chains of $[CdCl_2SO_4]^{2-}{}_n$ running along the *a*-axis. In the $[CdCl_2SO_4]^{2-}$ chain, $CdCl_4O_2$ octahedra share edges in a *trans*-fashion *via* their Cl atoms, and the SO_4 tetrahedra are grafted on to the chain in a symmetrical bridge. The Cd atoms are six-coordinated by four Cl and two O neighbors, with the Cd–Cl bond distances in the range 2.5827(11)−2.6425(12) Å [$(Cd–Cl)_{av}$ = 2.6103(2)Å] and Cd–O bond distances in the range 2.312(3)–2.338(3) Å [$(Cd–O)_{av}$ = 2.325Å]. The *cis*-O/Cl–Cd(1)–O/Cl bond angles are between 85.32(4) and 98.30(4)° [(*cis*-O/Cl–Cd(1)–O/Cl)$_{av}$ = 90.00(8)°] and the *trans*-O/Cl–Cd(1)–O/Cl bond angles are between 175.67(4) and 179.46(11)° [(*trans*-O/Cl–Cd(1)–O/Cl)$_{av}$ = 177.04(6)°]. Thus the $CdCl_4O_2$ octahedron

is nearly perfect. Selected bond distances are listed in Table 2. The S–O bond distances in the SO_4 tetrahedron are in the range 1.441(3) to 1.472(3) Å [$(S(1)–O)_{av}$ = 1.457(7) Å and $(S(2)–O)_{av}$ = 1.463(7) Å], with the O–S–O bond angles in the range 107.2(2)–112.1(2)°, [$(O–S(1)–O)_{av}$ = 109.46(6)° and $(O–S(2)–O)_{av}$ = 109.45°]. The Cd atom forms two Cd–O–S bonds to the crystallographically distinct S(1) atoms and four Cd–Cl–Cd bonds with the two crystallographically unique Cd(1) atoms. Similarly, S(1) form two S–O–Cd bonds with two Cd(1) atom and two terminal S=O bonds. S(2), on the other hand, has only terminal oxygen. The *trans* orientation of the bridging Cl atom creates a zigzag {–Cd–μ-Cl–Cd–μ-Cl–Cd–} backbone to the linear chain of $CdCl_4O_2$ octahedra and also creates a pair-wise canting of the Cd–O bonds as shown in Fig. 2(b). The pair-wise canting of the Cd–O bonds in the two adjacent Cd sites of the edge-shared $CdCl_4O_2$ octahedron allows the sulfate moiety to bridge symmetrically as shown in Fig. 2(c), thus forming a synthetic analogue of the linarite chain.[11]

The 1D chains along the *a*-axis in **I** are arranged parallel to one another in the *ac*-plane to form a layer-like arrangement [Fig. 3]. The layers are held together by the hydrogen bonded assembly of the diprotonated amine molecules, water molecules

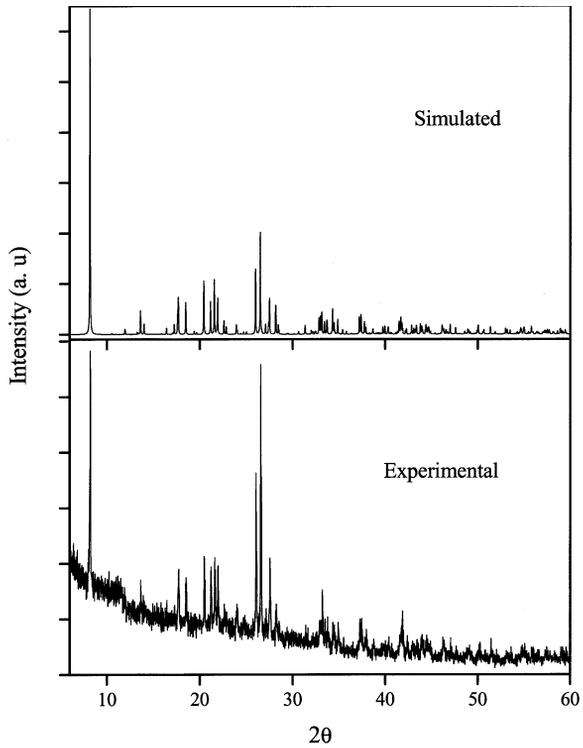

Fig. 1 The simulated and experimental powder X-ray pattern for compound $[H_3N(CH_2)_3NH_3][Cd_2(H_2O)_2(SO_4)_3]$, **IV**.

Table 2 Selected bond distances for $[C_2N_2H_{10}]_2[CdCl_2(SO_4)][SO_4]\cdot H_2O$, **I**

Cd(1)–O(1)	2.312(3)	S(1)–O(1)#2	1.466(3)
Cd(1)–O(2)	2.338(3)	S(1)–O(2)	1.472(3)
Cd(1)–Cl(1)	2.6092(11)	S(1)–O(3)	1.441(3)
Cd(1)–Cl(1)#1	2.5827(11)	S(1)–O(4)	1.452(3)
Cd(1)–Cl(2)	2.6425(12)	S(2)–O(5)	1.450(3)
Cd(1)–Cl(2)#2	2.6069(12)	S(2)–O(6)	1.464(3)
Cl(2)–Cd(1)#1	2.6069(12)	S(2)–O(7)	1.471(4)
Cl(1)–Cd(1)#2	2.5827(11)	S(2)–O(8)	1.470(3)

Symmetry transformations used to generate equivalent atoms: #1 $x - 1/2, -y + 1/2, -z$. #2 $x + 1/2, -y + 1/2, -z$.

Table 3 The various hydrogen bonding interactions in compounds **I**–**IV**

D–H ··· A	D–H/Å	H ··· A/Å	D ··· A/Å	D–H ··· A/°
I				
N(1)–H(1) ··· O(3)	0.889(6)	1.924(5)	2.771(5)	158.7(4)
N(1)–H(2) ··· O(5)	0.890(7)	2.173(6)	3.040(6)	164.6(4)
N(1)–H(3) ··· O(100)	0.891(7)	1.980(7)	2.809(7)	154.3(4)
N(2)–H(8) ··· O(8)	0.889(6)	1.950(5)	2.816(5)	164.3(4)
N(2)–H(9) ··· O(2)	0.890(5)	1.960(5)	2.847(5)	174.1(4)
N(2)–H(10) ··· O(1)	0.890(6)	2.018(5)	2.857(5)	156.5(5)
N(3)–H(12) ··· O(6)	0.890(6)	1.799(5)	2.672(5)	166.3(5)
N(3)–H(13) ··· Cl(1)	0.889(6)	2.561(4)	3.406(4)	159.1(5)
N(4)–H(18) ··· O(7)	0.890(6)	1.891(5)	2.773(5)	170.7(5)′
N(4)–H(19) ··· O(4)	0.889(6)	2.069(5)	2.772(5)	135.2(5)
N(4)–H(20) ··· O(8)	0.890(6)	1.911(5)	2.770(5)	161.8(5)
O(100)–H(21) ··· O(3)	0.80(7)	2.08(7)	2.881(7)	179(7)
O(100)–H(22) ··· O(5)	0.79(7)	2.07(7)	2.812(7)	155(6)
II				
N(1)–H(1) ··· O(2)	0.910(6)	1.783(6)	2.639(6)	155.6(6)
III				
N(1)–H(1) ··· O(2)	0.910(6)	1.843(7)	2.671(7)	150.1(6)
C(2)–H(4) ··· O(2)	0.970(6)	2.586(7)	3.477(7)	152.8(5)
IV				
N(1)–H(1) ··· O(7)	0.890(9)	2.093(9)	2.951(9)	161.7(8)′
N(1)–H(2) ··· O(6)	0.891(10)	2.123(10)	2.951(10)	154.3(8)′
N(1)–H(3) ··· O(12)	0.890(9)	2.591(9)	3.348(9)	143.5(7)
N(1)–H(3) ··· O(13)	0.890(9)	2.124(9)	2.952(9)	154.4(8)′
N(2)–H(11) ··· O(11)	0.889(10)	2.506(9)	3.306(9)	149.9(7)
N(2)–H(11) ··· O(13)	0.889(10)	2.281(9)	3.042(9)	143.5(7)′
N(2)–H(12) ··· O(2)	0.890(9)	2.129(8)	3.006(8)	168.3(8)
O(5)–H(13) ··· O(12)	0.92(8)	1.92(8)	2.799(9)	160(6)′
O(5)–H(14) ··· O(14)	0.76(12)	2.04(12)	2.787(9)	168(13)
O(6)–H(16) ··· O(14)	1.09(15)	1.74(15)	2.777(8)	156(13)
O(6)–H(17) ··· O(11)	0.85(8)	1.85(8)	2.686(8)	168(8)
C(1)–H(4) ··· O(10)	0.970(11)	2.567(9)	3.333(9)	135.9(8)
C(3)–H(8) ··· O(13)	0.969(12)	2.374(10)	3.319(10)	164.9(9)
C(3)–H(9) ··· O(12)	0.970(14)	2.412(11)	3.279(11)	148.4(8)

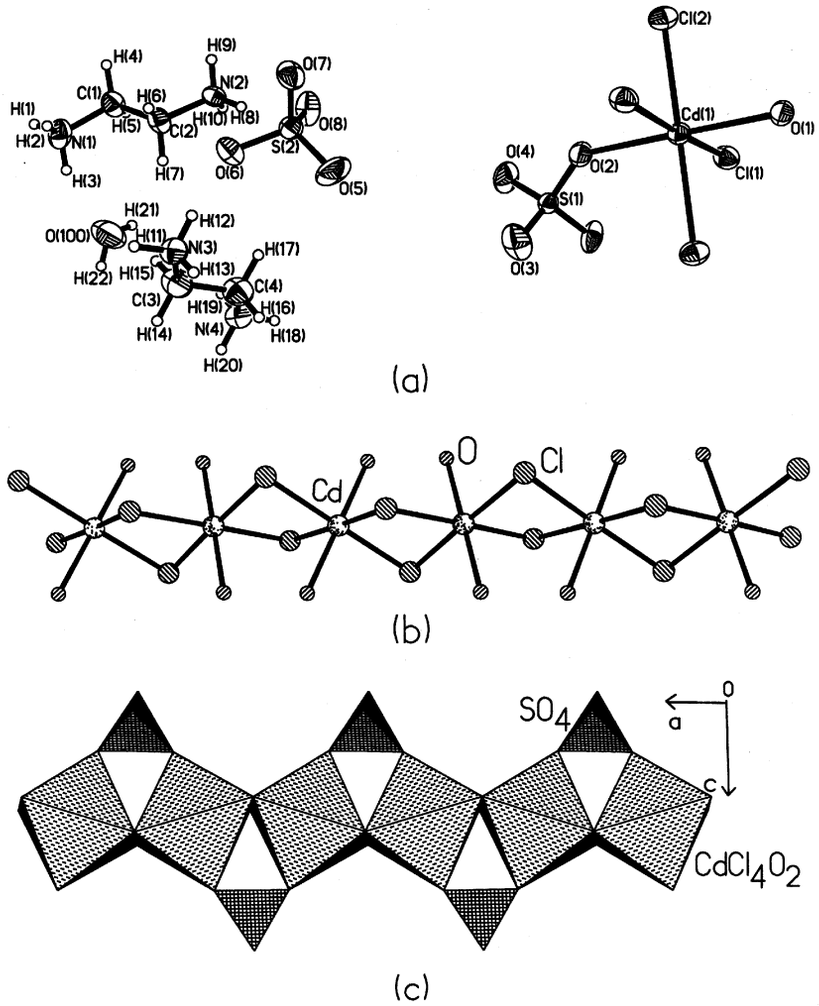

Fig. 2 (a) ORTEP[10] plot of $[H_3N(CH_2)_2NH_3]_2[CdCl_2(SO_4)][SO_4]\cdot H_2O$, **I**. The asymmetric unit is labeled. Thermal ellipsoids are given at 50% probability. (b) The pair-wise canting of the Cd–O bonds gives rise to a helical arrangement of the {–Cd–μ-Cl–Cd–μ-Cl–Cd–} backbone in **I**, along the *b*-axis. (c) The inorganic part of **I**, $[CdCl_2SO_4]^{2-}{}_n$, showing the linarite-type chain along the *b*-axis.

Table 4 Selected bond distances for $[C_6N_2H_{14}][CdBr_2(SO_4)]$, **II**

Cd(1)–O(1)#1	2.291(5)	Cd(1)–O(1)	2.291(5)
Cd(1)–O(1)#2	2.291(4)	Cd(1)–O(1)#3	2.291(4)
Cd(1)–Br(1)#2	2.7669(4)	Cd(1)–Br(1)#4	2.7669(4)
Cd(1)–Br(1)#5	2.7669(4)	Cd(1)–Br(1)	2.7669(4)
S(1)–O(2)	1.440(5)	S(1)–O(2)#5	1.440(5)
S(1)–O(1)#6	1.465(5)	S(1)–O(1)#5	1.465(5)
S(1)–O(1)#3	1.465(5)	S(1)–O(1)	1.465(5)
Br(1)–Cd(1)#1	2.7669(4)		

Symmetry transformations used to generate equivalent atoms: #1 x, $-y$, $-z$. #2 $-x$, $-y$, $-z$. #3 $-x$, y, z. #4 x, $-y$, $z-1/2$. #5 $-x$, y, $-z+1/2$. #6 x, y, $-z+1/2$.

Table 5 Selected bond distances for $[C_6N_2H_{14}][CdCl_2(SO_4)]$, **III**

Cd(1)–O(1)#1	2.275(5)	Cd(1)–O(1)#2	2.275(5)
Cd(1)–O(1)#3	2.275(5)	Cd(1)–O(1)	2.275(5)
Cd(1)–Cl(1)#4	2.6415(9)	Cd(1)–Cl(1)	2.6415(9)
Cd(1)–Cl(1)#1	2.6415(9)	Cd(1)–Cl(1)#5	2.6416(9)
S(1)–O(2)#4	1.437(5)	S(1)–O(2)	1.437(5)
S(1)–O(1)#6	1.466(5)	S(1)–O(1)#4	1.466(5)
S(1)–O(1)#3	1.466(5)	S(1)–O(1)	1.466(5)
Cl(1)–Cd(1)#3	2.6415(9)		

Symmetry transformations used to generate equivalent atoms: #1 $-x$, $-y$, $-z$. #2 x, $-y$, $-z$. #3 $-x$, y, z. #4 $-x$, y, $-z+1/2$. #5 x, $-y$, $z-1/2$. #6 x, y, $-z+1/2$.

and free sulfate moieties located in the interlamellar space, to form the 3D assembly [Fig. S1, ESI †]. Such isolated oxo anions in the interlamellar space have been observed in sulfate minerals

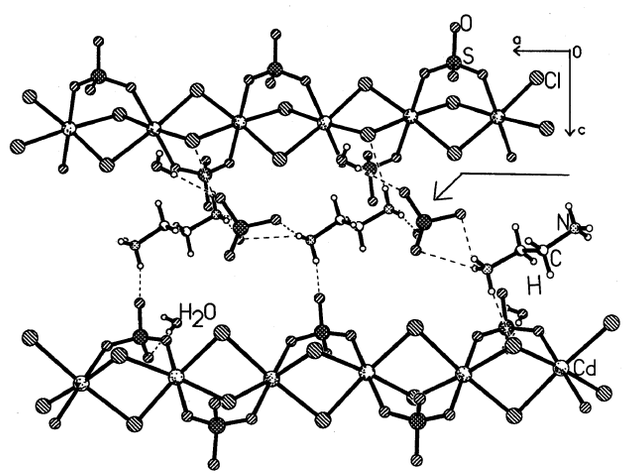

Fig. 3 The structure of **I** in the *ac*-plane. Note the orientations of the amine molecules, the intercalated sulfate ion (shown by an arrow) and the water molecules occupying positions in between the chains. Dotted lines represent hydrogen bond interactions.

with layered structures[12] and in organically templated layered phosphates.[13] The free sulfate ions interact with the diprotonated amine and water molecules through N–H ··· O and O–H ··· O hydrogen bonds. Apart from N–H ··· O and O–H ··· O interactions, there is also an N–H ··· Cl interaction. Metal-bound Cl atoms acting as hydrogen bond acceptors have

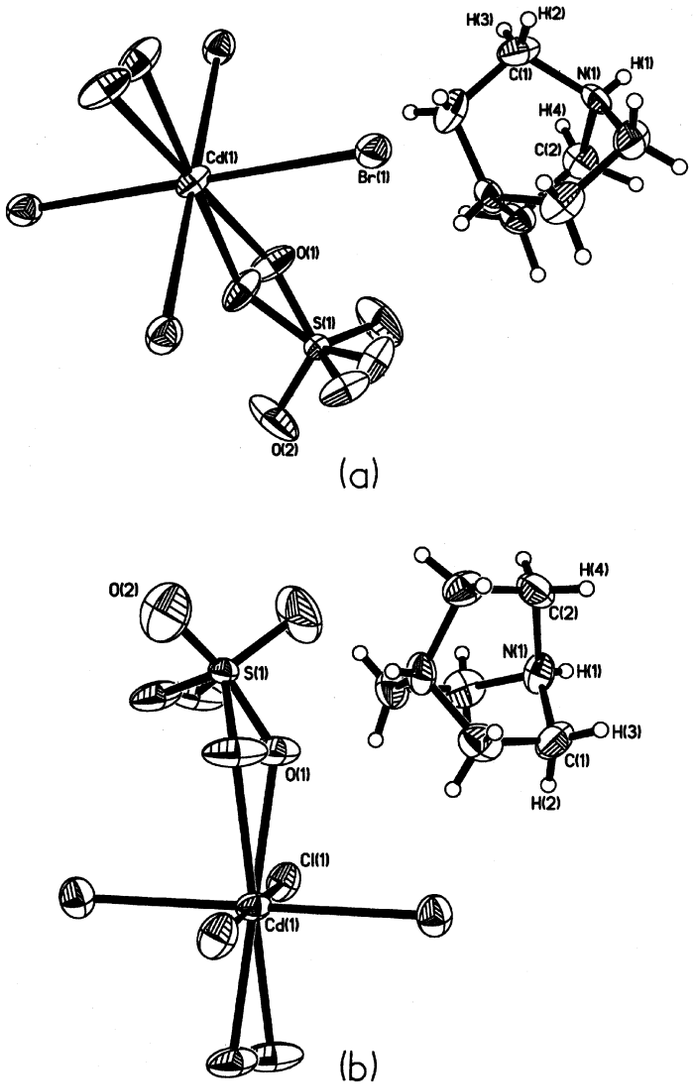

Fig. 4 (a) ORTEP plot of $[HN(CH_2)_6NH][CdBr_2(SO_4)]$, **II**. The asymmetric unit is labeled. Thermal ellipsoids are given at 50% probability. (b) ORTEP plot of $[HN(CH_2)_6NH][CdCl_2(SO_4)]$, **III**. The asymmetric unit is labeled. Thermal ellipsoids are given at 50% probability.

been recognized previously.[14] The various hydrogen bond interactions in **I** are listed in Table 3.

$[HN(CH_2)_6NH][CdBr_2(SO_4)]$, II and $[HN(CH_2)_6NH][CdCl_2(SO_4)]$, III

The asymmetric units of compounds **II** and **III** contain eight non-hydrogen atoms out of which five belong to the inorganic framework and three belong to the organic molecule [Fig. 4]. The inorganic framework structures of **II** and **III** are identical having the same linarite topology as in **I**. The only difference between **II** and **III** is in the bridging atom between the CdX_4O_2 octahedra, being Br in the case of **II** and Cl in **III**. Both **II** and **III** have disorder in one of the oxygen sites O(1) as shown in Fig. 5(a). The amine 1,4-diazabicyclo[2.2.2]octane (DABCO) is diprotonated in both **II** and **III**. In **II**, the Cd–Br and Cd–O distances are 2.7669(4) and 2.291(5) Å respectively. The S–O bond distances range from 1.440(5) to 1.465(5) Å, with an average of 1.45(6) Å. In **III**, the Cd–Cl and Cd–O distances are 2.6415(9) Å and 2.275(5) Å respectively. The S–O bond distances range from 1.437(5) to 1.466(5) Å with an average of 1.452 Å. The longer Cd–X distance in **II** results in a larger volume relative to **III**. Selected bond distances for **II** and **III** are listed in Tables 4 and 5 respectively.

The individual chains in **II** and **III** are held together by hydrogen bond interactions, involving the diprotonated amine to form the layered structure [Fig. S2, ESI †]. The layers are stacked one over the other along the *a*-axis with the diprotonated DABCO molecules in the interlayer space. Hydrogen bonding involving the chain–template interaction contributes to the stability of the 3D crystalline assembly. This creates a cavity, along the *c*-axis as shown in Fig. 5(b). Such pseudo channels resemble those in organic hydrogen-bonded structures.[15] The various hydrogen-bonding interactions in **II** and **III** are listed in Table 3.

$[H_3N(CH_2)_3NH_3][Cd_2(H_2O)_2(SO_4)_3]$, IV

The asymmetric unit of **IV** contains 24 non-hydrogen atoms out of which 19 belong to the inorganic framework and 5 belong to the extra framework amine molecule [Fig. 6(a)]. There are two crystallographically distinct Cd atoms and three S atoms, with both the Cd atoms having octahedral geometry. The Cd(1) atom is octahedrally coordinated to six oxygens, of which four are from the corner-sharing sulfate ions and two are from the terminal water molecules $[Cd(1)O_4(H_2O)_2]$. On the other hand, Cd(2) is octahedrally coordinated to six oxygens, of which four are from the corner-sharing sulfate ions and two are from the edge-sharing sulfate ions $[Cd(2)O_6]$. The $S(1)O_4$ and $S(3)O_4$ tetrahedra shares their four vertexes with cadmium octahedra to form four-connected tetrahedra which is rather unusual.[12]The S(2) atom is tetrahedrally coordinated to four oxygens, of which two share edges with cadmium [Cd(2)] octahedra and the remaining are terminal S=O groups. The

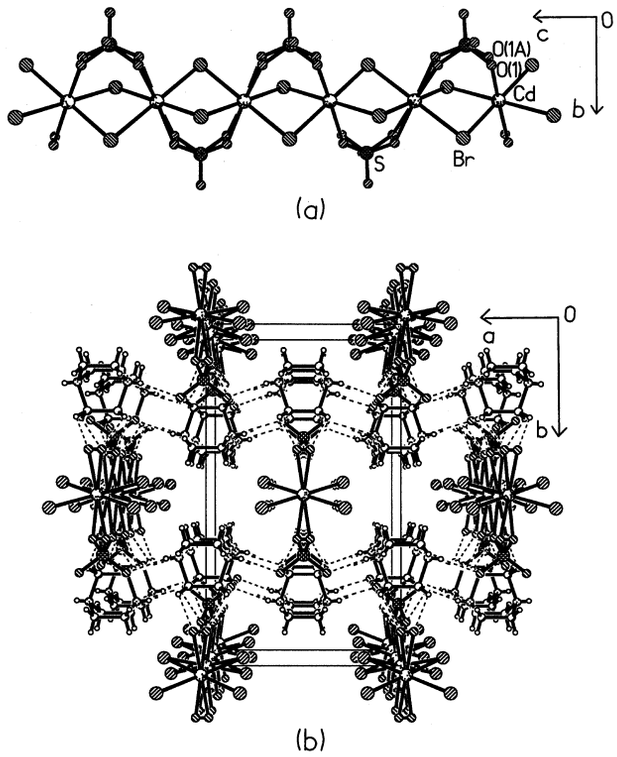

Fig. 5 (a) The inorganic part of $[HN(CH_2)_6NH][CdBr_2(SO_4)]$, **II**, along the *a*-axis. Note the disorder in the structure. (b) Projection of **II** along [001] showing pseudo channels. Hydrogen bonds are shown as dotted lines.

inorganic layer is built up of four-membered rings formed by two CdO_6 octahedra and two SO_4tetrahedra linked through vertices [Fig. 6(b)]. The connectivity between the four-membered rings leads to the formation of a four-membered ladder with strictly alternating CdO_6 octahedra and SO_4 tetrahedra, the ladders being fused in the *ab*-plane to form the 2D framework of the inorganic layer [Fig. 7(a) and Fig. S3, ESI †]. The Cd(1) and Cd(2) atoms are surrounded by the four four-membered rings with direct linkage to four SO_4 tetrahedra. Similarly, the S(1) atom is surrounded by the four four-membered rings with direct linkage to four CdO_6 octahedra [Fig. 6(c)–(e)]. The remaining coordination of the Cd octahedron is satisfied by the edge-sharing SO_4 in Cd(2) and by the two water molecules in Cd(1).

The coordination environments of the various sites in **IV** can be represented by the Schläfli symbol[16] which specifies the connectivity of the various vertex-linked polygons. According to the Schläfli notation, the coordination environment for Cd and S can be represented as $\mathbf{4^4}$. Hence the circuit symbol,[17] which enumerates the smallest T-atom loop pathways, can be written as $\mathbf{4^4}$ for all tetrahedral and octahedral atoms. This type of octahedral–tetrahedral atom configuration [Fig 7(b)] has not been previously reported for any other open-framework solids. Bu *et al.*[18] have previously observed the four-connected 2D tetrahedral atom configuration in zinc arsenate. In known cases where lamellar structures are formed from tetrahedral atoms, there are always interruptions and the resulting structures, even if polymeric, are not completely 4-connected.[19] The conversion of a $\mathbf{4^4}$ 2D net into a 3D net with 4-fold helices is reported to yield a cristobalite net.[20] This familiar net occurs most notably in cubic close packing (fcc), in simple cubic and in body-centered cubic three-dimensional arrays.[16] The nets in **IV** are stacked one over the other along the *c*-axis in an *AAAA* fashion and the diprotonated 1,3-diaminopropane (DAP) molecules occupy the interlayer space. The layers in **IV** are four polyhedra in thickness as a consequence of the projection of the pendant apices of the sulfate tetrahedra above and below the plane. These amine molecules interact strongly with the inorganic framework through N–H ··· O hydrogen bonding to stabilize the 3D structure as shown in Fig. 7(c). The framework stoichiometry of $[Cd_2(H_2O)_2(SO_4)_3]$ has a charge of −2 which is balanced by the diprotonated DAP resulting in the formula $[DAPH_2][Cd_2(H_2O)_2(SO_4)_3]$. Hydrogen bonding involving layer–layer (O–H ··· O) and layer–template (N–H ··· O and C–H ··· O) interactions contributes to the stability of the 3D structure.

Table 6 Selected bond distances and angles for $[C_3N_2H_{16}][Cd_2(H_2O)_2(SO_4)_3]$, **IV**

Cd(1)–O(1)	2.224(5)	Cd(1)–O(4)	2.293(5)
Cd(1)–O(3)	2.286(5)	Cd(1)–O(6)	2.339(5)
Cd(1)–O(5)	2.311(6)	Cd(2)–O(8)	2.268(4)
Cd(2)–O(7)	2.233(5)	Cd(2)–O(10)	2.273(4)
Cd(2)–O(9)	2.270(5)	Cd(2)–O(12)	2.545(6)
Cd(2)–O(11)	2.334(5)	S(1)–O(1)#1	1.468(5)
S(1)–O(4)	1.472(5)	S(1)–O(8)	1.476(5)
S(1)–O(9)#2	1.481(5)	S(2)–O(13)	1.451(5)
S(2)–O(12)	1.461(5)	S(2)–O(14)	1.469(5)
S(2)–O(11)	1.504(5)	S(3)–O(10)#3	1.458(5)
S(3)–O(3)#4	1.482(5)	S(3)–O(2)#1	1.482(5)
S(3)–O(7)	1.483(5)	O(1)–S(1)#1	1.468(5)
O(2)–S(3)#1	1.482(5)	O(3)–S(3)#5	1.482(5)
O(9)–S(1)#2	1.481(5)	O(10)–S(3)#3	1.458(5)
Cd(1)–O(2)	2.274(5)		
O(1)–Cd(1)–O(4)	90.4(2)	O(3)–Cd(1)–O(4)	90.5(2)
O(2)–Cd(1)–O(5)	90.2(2)	O(4)–Cd(1)–O(5)	84.9(2)
O(2)–Cd(1)–O(6)	89.9(2)	O(4)–Cd(1)–O(6)	84.6(2)
O(7)–Cd(2)–O(9)	105.4(2)	O(7)–Cd(2)–O(10)	99.8(2)
O(9)–Cd(2)–O(10)	81.1(2)	O(1)–Cd(1)–O(3)	101.2(2)
O(8)–Cd(2)–O(11)	86.9(2)	O(10)–Cd(2)–O(11)	89.7(2)
O(8)–Cd(2)–O(12)	77.3(2)	O(10)–Cd(2)–O(12)	87.1(2)
O(7)–Cd(2)–O(8)	96.3(2)	O(8)–Cd(2)–O(9)	90.8(2)
O(8)–Cd(2)–O(10)	163.4(2)	O(7)–Cd(2)–O(11)	116.0(2)
O(9)–Cd(2)–O(11)	138.6(2)	O(7)–Cd(2)–O(12)	171.0(2)
O(9)–Cd(2)–O(12)	81.3(2)	O(11)–Cd(2)–O(12)	57.9(2)
O(1)–Cd(1)–O(2)	95.0(2)	O(1)#1-S(1)–O(4)	108.9(3)
O(2)–Cd(1)–O(3)	92.4(2)	O(4)–S(1)–O(8)	107.4(3)
O(2)–Cd(1)–O(4)	173.3(2)	O(4)–S(1)–O(9)#2	110.5(3)
O(1)–Cd(1)–O(5)	100.8(2)	O(13)–S(2)–O(12)	110.5(3)
O(3)–Cd(1)–O(5)	157.5(2)	O(12)–S(2)–O(14)	110.5(3)
O(1)–Cd(1)–O(6)	175.0(2)	O(12)–S(2)–O(11)	106.0(3)
O(3)–Cd(1)–O(6)	79.4(2)	O(10)#3–S(3)–O(3)#4	111.6(3)
O(5)–Cd(1)–O(6)	78.2(3)	O(3)#4–S(3)–O(2)#1	110.7(3)
O(2)#1–S(3)–O(7)	109.9(3)	O(3)#4–S(3)–O(7)	108.3(3)
O(1)#1–S(1)–O(8)	109.7(3)	O(1)#1–S(1)–O(9)#2	110.1(3)
O(8)–S(1)–O(9)	110.2(3)	O(13)–S(2)–O(14)	111.6(3)
O(13)–S(2)–O(11)	108.8(3)	O(14)–S(2)–O(11)	109.2(3)
O(10)#3–S(3)–O(2)#1	107.4(3)	O(10)#3–S(3)–O(7)	109.0(3)

Symmetry transformations used to generate equivalent atoms: #1 $-x$, $-y+1$, $-z+1$. #2 $-x-1$, $-y+1$, $-z+1$. #3 $-x-1$, $-y$, $-z+1$. #4 x, $y-1$, z. #5 x, $y+1$, z.

The Cd–O bond lengths in **IV** range from 2.224(5) to 2.545(6), $[Cd(1)–O]_{av}$ = 2.287(8) and $[Cd(2)–O]_{av}$ = 2.320(5) Å. The *cis*-O–Cd–O bond angles are between 57.9(2) and 116.0(2)° [(*cis*-O–Cd(1)–O)$_{av}$ = 89.79° and (*cis*-O–Cd(2)–O)$_{av}$ = 89.13°] and the *trans*-O–Cd–O bond angles are between 138.6(2) and 175.0(2)° [(*trans*-O–Cd(1)–O)$_{av}$ = 168.6° and (*trans*-O–Cd(2)–O)$_{av}$ = 157.6(6)°]. The bond angle and bond distance values indicate that both Cd(1) and Cd(2) octahedra are highly distorted. The tetrahedral S–O bond distances are in the range 1.451(5) to 1.504(5) Å with average S(1)–O, S(2)–O and S(3)–O distances of 1.474(2), 1.471(2) and 1.476(2) Å respectively. The O–S–O bond angles are in the range 106.0(3)–111.6(3)° [(O–S(1)–O)$_{av}$ = 109.4(6)°, (O–S(2)–O)$_{av}$ = 109.4(3)° and (O–S(3)–O)$_{av}$ = 109.4(8)°]. Values of selected bond distances and angles in **IV** are listed in Table 6, and the various hydrogen bond interactions in Table 3.

Thermal behavior

The TGA curves of **I**–**IV** given in Fig. 8 show distinct mass losses. In **I** there is a three-step weight loss corresponding to the

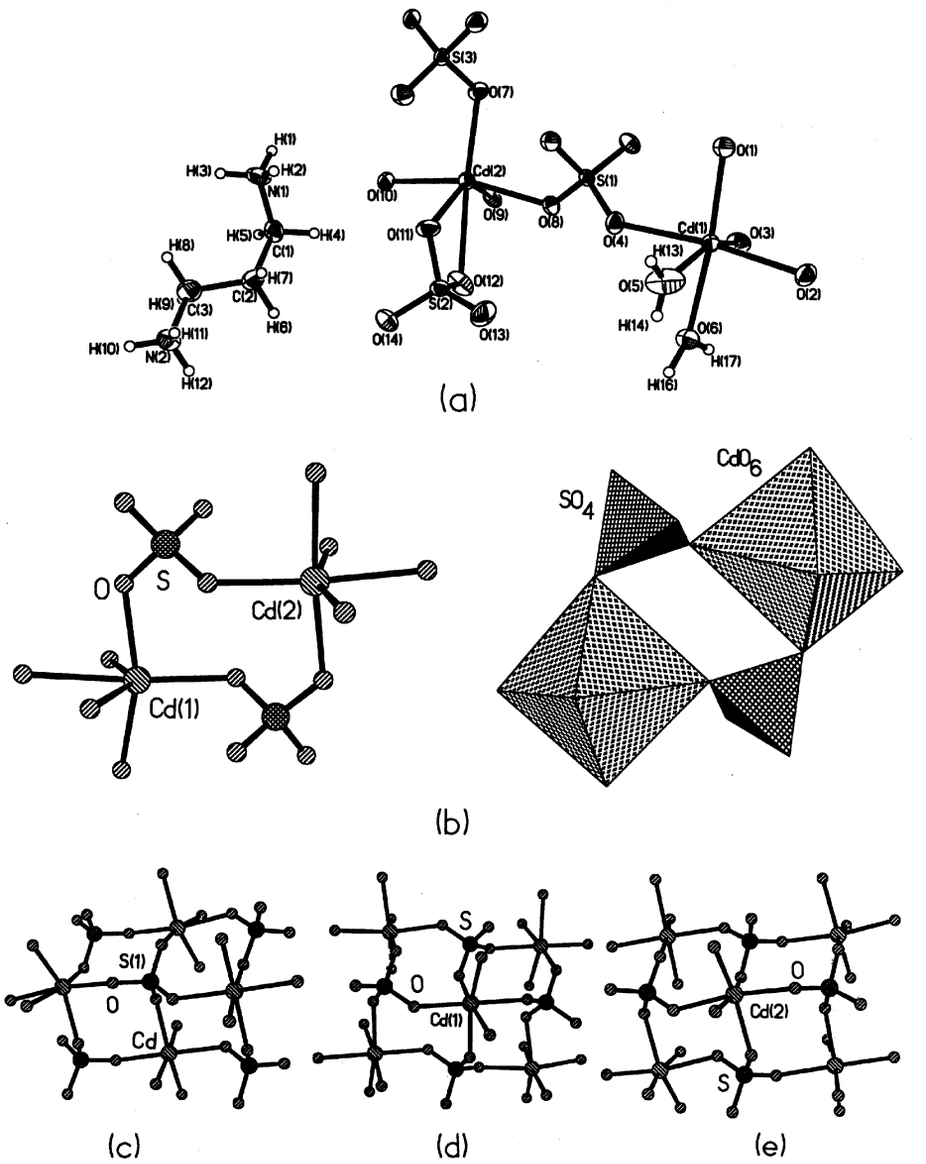

Fig. 6 (a) ORTEP plot of $[H_3N(CH_2)_3NH_3][Cd_2(H_2O)_2(SO_4)_3]$, **IV**. The asymmetric unit is labeled. Thermal ellipsoids are given at 50% probability. (b) Ball and stick and polyhedral structures of the four-membered ring in **IV**. (c)–(e) Ball and stick structures showing the coordination environment of the $S(1)O_4$ tetrahedra, $Cd(1)O_6$ octahedra and $Cd(2)O_6$ octahedra in **IV** respectively. Note both Cd and S are located in the middle of an eight-membered ring.

loss of water molecule at 100 °C [obs = 2.3%, calc = 3.4%], the amine molecules and the free sulfate (H_2O + SO_3) at 300 °C [obs = 58.2%, calc = 61%], followed by the removal of the remaining H_2O and Cl_2 in the range 400 °C to 850 °C [obs = 16.5%, calc = 16.8%]. The powder X-ray diffraction pattern (PXRD) of the decomposed sample corresponds to metallic Cd (JCPDS file card No. 05–0674). **II** shows a sharp two-step weight loss around 330 °C and 600 °C corresponding to the loss of DABCO and one HBr molecule [obs = 40%, calc = 39.6%] and one SO_3 and one HBr molecule [obs = 38%, calc = 33%] respectively. The PXRD pattern of the sample heated at 800 °C diffracts weakly and could not be characterized. There is a sharp weight loss of DABCO and HCl molecules at ≈330 °C [obs = 44%, calc = 46%], and at ≈640 °C the loss of O_2 in **III**, resulting in CdS. The PXRD pattern of the sample heated at 800 °C corresponds to CdS (greennockite) (JCPDS file card No. 41–1049). The low temperature decomposition of **II** and **III** compared to **I** can be related to the absence of N–H ··· X interactions in **II** and **III**. The TGA curve of **IV** reveals the loss of water at 200 °C [obs = 6.05%, calc = 5.75%], the loss of DAP, SO_2 and H_2O at 350 °C [obs = 23.7%, calc = 24.95%], followed by the loss of the remaining SO_3 in the 550–750 °C range. The powder X-ray diffraction pattern of the decomposed sample of **IV** corresponds to CdO (monteporite) (JCPDS file card No. 05–0640), indicating the collapse of the framework upon removal of the amine molecule. The powder XRD patterns of the sample heated to 280 °C indicates the structure is intact even though the bonded water molecules have been eliminated. It is relevant to say at this stage that the cadmium octahedra may be transforming to tetrahedra at high temperature (280 °C) in **IV**.

Discussion

The three new linarite type chains and the layered cadmium sulfate found in the present study enlarge the family of organically templated sulfates. Several of the structural features in compound **I**–**IV** are worthy of attention. The infinite chains of $[M(TO_4)\varphi]$ stoichiometry (M = octahedral metal, T = tetrahedral element, φ = an anionic ligand, example: OH, F, Cl, Br or I) in the linarite group of minerals are rather rare.[11] To our knowledge, **II** is the first cadmium bromosulfate with an extended structure. Our attempts to prepare hydroxo (OH)

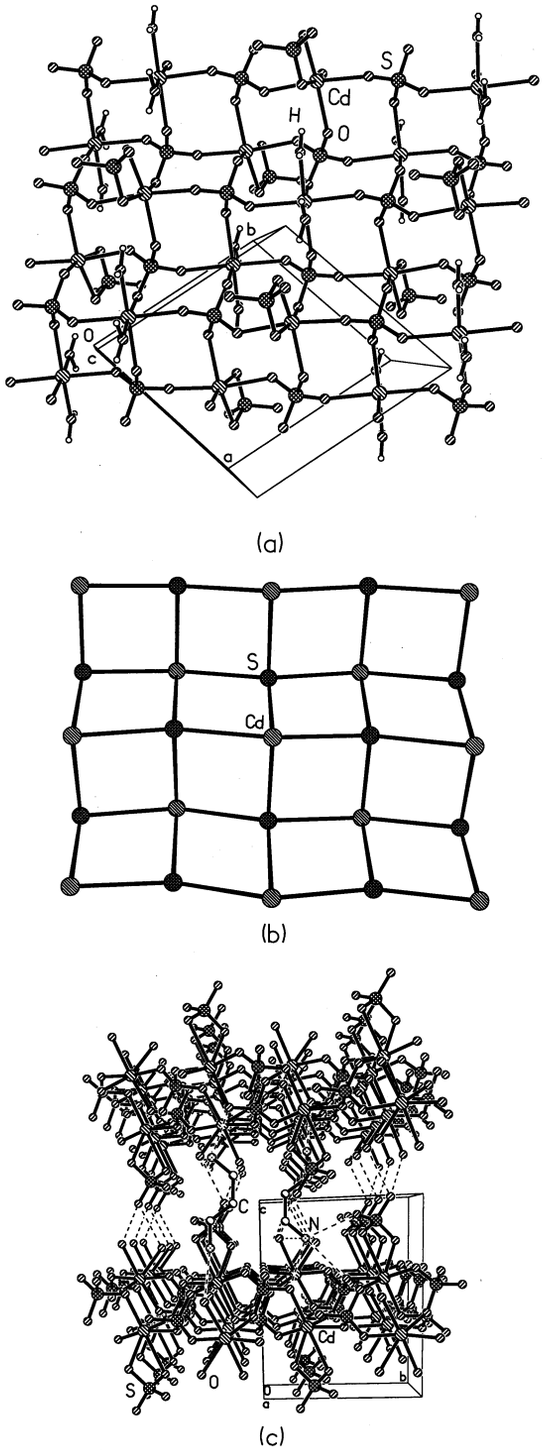

Fig. 7 (a) Ball and stick view of **IV** in the *ab*-plane showing the fusion of the four-membered ring ladders to form the layered architecture. Note the presence of four-connected SO_4 tetrahedron and edge sharing SO_4 tetrahedron. (b) The T-atom (Cd, S) connectivity in **IV** showing a 4^4 plane net. (c) View down the crystallographic *a*-axis showing the packing of layers in **IV**. Note the pillaring role of diprotonated DAP molecules and layer–layer hydrogen-bonding interactions. Hydrogen atoms are omitted for clarity.

and iodo (I) analogues of the linarite chain have not yet been successful. The occurrence of linarite type chains in various synthetic organically templated phosphates such as in $FePO_4$[21] and $GaPO_4$[22] and in the minerals, tsumcorite, $Pb[(Zn,Fe^{3+})(AsO_4)(H_2O,OH)]_2$,[11c,23] bermanite, $Mn^{2+}[Mn^{3+}(PO_4)(OH)]_2(H_2O)_4$[11c,24] and natrochalcite, $Na[Cu^{2+}{}_2(OH)(H_2O)(SO_4)_2]$,[25] indicates that it may be an important building unit involved in the formation of higher dimensional structures. Recently such

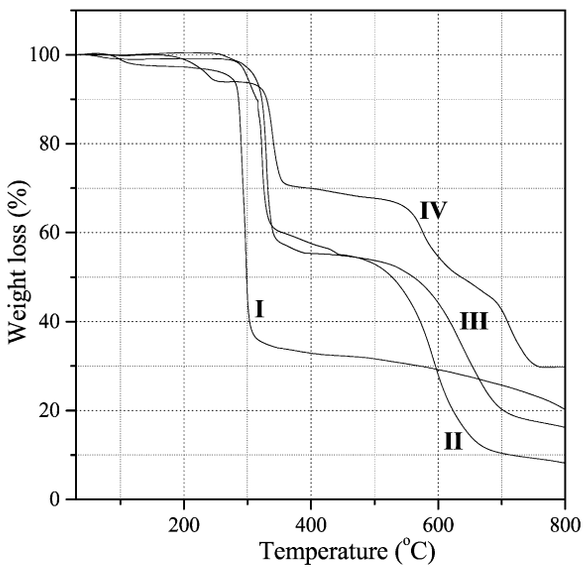

Fig. 8 TGA curves of compounds **I**–**IV**.

one-dimensional solids[3,26] have been recognized as important intermediates in the formation of higher dimensional structures in zinc and gallium phosphates. In this regard, the isolation of such chains in the organically templated sulfate family merits special mention.

The topology of layered structures is usually viewed based on the connectivity of polyhedral atoms. Both four-connected 3D nets and three-connected 2D nets are common among the known structures.[17] To our knowledge, there is no example of a structure in which octahedral–tetrahedral atoms form four-connectivity of the tetrahedral unit in a 2D net. The unique features of **IV** are the presence of the four-connected SO_4 tetrahedron and of the edge-sharing of SO_4 tetrahedra in the 2D net. Edge-sharing sulfates are dominant in compounds containing polyhedra with more than six vertices, as in gypsum, where the CaO_8 dodecahedron shares edges with the sulfate tetrahedra.[12] The structure of **IV** involves strictly alternating CdO_6 and SO_4 connectivity. The presence of four-connected SO_4 tetrahedra suggests that it is desirable to investigate the organically templated sulfate family for new structures. It is likely that 3D structures will be formed in the presence of different amines under appropriate conditions.

References

1 (*a*) D. W. Breck, *Zeolite Molecular Sieves*, Wiley, New York, 1974; W. M. Meier, D. H. Oslen and C. Baerlocher, *Atlas of Zeolite Structure Types*, Elsevier, London, 1996.
2 A. K. Cheetham, G. Férey and T. Loiseau, *Angew. Chem.*, 1999, **111**, 3466 (*Angew. Chem., Int. Ed.*, 1999, **38**, 3268–3292).
3 C. N. R. Rao, S. Natarajan, A. Choudhury, S. Neeraj and A. A. Ayi, *Acc. Chem. Res.*, 2001, **34**, 80.
4 (*a*) A. Choudhury, J. Krishnamoorthy and C. N. R. Rao, *Chem. Commun.*, 2001, 2610; (*b*) A. Choudhury, D. Udaya Kumar and C. N. R. Rao, *Angew. Chem.*, 2002, **41**, 158 and references therein; (*c*) W. T. A. Harrison, M. L. F. Phillips, J. Stanchfield and T. M. Nenoff, *Angew. Chem.*, 2000, **112**, 3966–3968 (*Angew. Chem., Int. Ed.*, 2000, **39**, 3808).
5 (*a*) S. Neeraj, S. Natarajan and C. N. R. Rao, *Chem. Mater.*, 1999, **11**, 1390; (*b*) A. Choudhury, S. Neeraj, S. Natarajan and C. N. R. Rao, *J. Mater. Chem.*, 2001, **11**, 1537.
6 K. Jayaraman, A. Choudhury and C. N. R. Rao, *Solid State Sci.*, 2002, **4**, 413–422.
7 G. M. Sheldrick, SADABS, Siemens Area Detector Absorption Correction Program, University of Göttingen, Göttingen, Germany, 1994.
8 (*a*) G. M. Sheldrick, SHELXS-86, Program for crystal structure determination, University of Göttingen, 1986; (*b*) G. M. Sheldrick, *Acta Crystallogr., Sect. A*, 1990, **35**, 467.

9 G. M. Sheldrick, SHELXTL-PLUS, Program for Crystal Structure Solution and Refinement, University of Göttingen, Göttingen, Germany, 1993.
10 C. K. Johnson, ORTEP, Report ORNL-5138, Oak Ridge National Laboratory, Oak Ridge, TN, 1976.
11 (*a*) Von H.G. Bachmann and J. Zemann, *Acta Crystallogr.*, 1961, **14**, 747; (*b*) F.C. Hawthrone, *Z. Kristallogr.*, 1990, **192**, 1; (*c*) F.C. Hawthrone, *Acta Crystallogr., Sect. B*, 1994, **50**, 481.
12 F.C. Hawthrone, S. V. Krivovichev and P. C. Burns, *Rev. Miner. Geochem.*, 2000, **40**, 1.
13 (*a*) N. Simon, T. Loiseau and G. Ferey, *J. Mater. Chem.*, 1999, **9**, 585; (*b*) A. Choudhury, *Proc. Indian Acad. Sci. (Chem. Sci.)*, 2002, **114**, 93.
14 G. Aullón, D. Bellamy, L. Brammer, E. A. Bruton and A. G. Orpen, *Chem. Commun.*, 1998, 653.
15 A. Ranganathan, V. R. Pedireddi and C. N. R. Rao, *J. Am. Chem. Soc.*, 1999, **120**, 1752.
16 M. O'Keeffe and B. G. Hyde, *Acta Crystallogr.*, 1980, **295**, 553–618.
17 (*a*) J. V. Smith, *Am. Mineral.*, 1977, **62**, 703; (*b*) J. V. Smith, *Chem. Rev.*, 1988, **88**, 149 and references therein.
18 X. Bu, T. E. Gier and G. D. Stucky, *Chem. Commun.*, 1997, 2271.
19 J. R. D. DeBord, R. C. Haushaiter and J. Zubieta, *J. Solid State Chem.*, 1996, **125**, 270.
20 J. V. Smith, *Am. Mineral.*, 1979, **64**, 551.
21 (*a*) M. Cavellec, D. Riou and G. Férey, *Acta Crystallogr., Sect. C*, 1995, **51**, 2242; (*b*) J. R. D. DeBord, W. M. Reiff, R. C. Haushalter and J. Zubieta, *J. Solid State Chem.*, 1996, **125**, 186.
22 R. H. Jones, J. M. Thomas, H. Qisheng, M. B. Hursthouse and J. Chen, *J. Chem. Soc., Chem. Commun.*, 1991, 1520.
23 E. Tillmanns and W. Gebert, *Acta Crystallogr., Sect. B*, 1973, **29**, 2789.
24 A. R. Kampf and P.B. Moore, *Am. Mineral.*, 1976, **61**, 1241.
25 G. Giester and J. Zemann, *Z. Kristallogr.*, 1987, **179**, 431.
26 R. I. Walton, F. Millange, D. O'Hare, C. Paulet, T. Loiseau and G. Férey, *Chem. Mater.*, 2000, **12**, 1977.